

## Thermodynamic and Radiative Impact of the Correction of Sounding Humidity Bias in the Tropics

F. GUICHARD, D. PARSONS, AND E. MILLER

*NCAR/ATD, Boulder, Colorado*

(Manuscript received 11 August 1999, in final form 29 December 1999)

### ABSTRACT

Accurate measurements of atmospheric water vapor are crucial to many aspects of climate research and atmospheric science. This paper discusses some of the meteorological implications of a bias discovered in the measurement of water vapor in widely deployed radiosonde systems. This problem apparently arose in the early 1990s, and a correction scheme has been recently developed that intends to remove the bias. The correction scheme also includes improvements in the humidity measurements in the upper troposphere and near the surface. It has been applied to data taken during the Tropical Ocean and Global Atmosphere Coupled Ocean–Atmosphere Response Experiment (TOGA COARE).

The impact of the bias on the general stability of the tropical atmosphere to deep convection, as measured by the convective available potential energy (CAPE) and the convective inhibition (CIN), is quite large. On the basis of the uncorrected dataset, one might erroneously conclude that it is difficult to trigger deep convection over the region. When the correction is taken into account, the atmosphere over the tropical western Pacific becomes typically unstable to deep convection, with convective instability similar to that measured from aircraft in the vicinity of active convective systems.

Radiative fluxes are also significantly modified. For clear sky conditions, it is found that on average, the net surface radiative flux increases by  $4 \text{ W m}^{-2}$ , and the outgoing longwave flux decreases by more than  $2 \text{ W m}^{-2}$  due to the humidity correction. Under more realistic cloudy conditions, the differences are weaker but still significant. Changes in radiative fluxes are explained at first order by the precipitable water increase.

It is likely that such a dry bias would hide any modifications of the atmospheric water vapor associated with the increase of greenhouse gases.

### 1. Introduction

Atmospheric water vapor plays a crucial role in our climate. For example, it is well established that water vapor is the most important greenhouse gas in the atmosphere. Thus, the distribution of water vapor in the atmosphere strongly impacts the vertical profile of the radiative cooling and the magnitude of the radiative fluxes at the surface and the top of the atmosphere (TOA). In addition, the three-dimensional distribution of water vapor and how it interacts with the dynamics and thermodynamics of the earth's atmosphere directly control the three-dimensional distribution of clouds. Hence, it is not surprising that the vertical distribution of water vapor must be measured very accurately for observational studies aimed at investigating the climate of the earth and for estimating global climate change. Recent studies have shown that current measurement

strategies can result in large uncertainties in the observed radiative budget in the Tropics (Gutzler 1993) and have stressed the importance of improving the accuracy of water vapor measurements for detecting climate change (e.g., Harries 1997).

There is also a need for accurate measurement of water vapor for a variety of other problems in the atmospheric sciences, including boundary layer studies, atmospheric chemistry, hydrology, polar meteorology, and the prediction of severe weather events (Weckwerth et al. 1999). It has also been argued that advances in the quantitative prediction of convective rainfall in part hinge on our ability to improve the characterization of atmospheric water vapor (Emanuel et al. 1995; Dabberdt and Schlatter 1996). Accurate measurements of water vapor are also needed to estimate convective parameters (Crook 1996; Zipser and Johnson 1998), such as convective available potential energy (CAPE) and convective inhibition (CIN) (Colby 1983), which are useful for diagnosing global variations in convective intensity, convective structure, and the general stability of the atmosphere to convective overturning.

Partly due to the performance limitations of remote sensing techniques for water vapor (e.g., Smith and Ben-

---

*Corresponding author address:* Dr. Françoise Guichard, CNRM-GAME (CNRS & Météo-France), 42 av Coriolis, 31057, Toulouse Cedex, France.  
E-mail: francoise.guichard@meteo.fr

jamin 1993; Weckwerth et al. 1999), the radiosonde is still an important component of the global observing network. Radiosondes, in fact, are still used to “calibrate” some remote sensing techniques. A discussion of the errors in radiosonde measurements taken during the Tropical Ocean and Global Atmosphere Coupled Ocean–Atmosphere Response Experiment (TOGA COARE) can be found in Zhang and Chou (1999). In addition to the error sources discussed by Zhang and Chou (1999), a dry bias was discovered in radiosonde measurements of humidity during TOGA COARE (Zipser and Johnson 1998; Lucas and Zipser 2000). The causes for this bias have been identified, and a correction procedure has been designed based on extensive laboratory and atmospheric data (Barr and Betts 1997; Cole and Miller 1999). This correction generally leads to a moistening of the measurement over the depth of the troposphere. The bias is not limited to soundings taken during TOGA COARE. Instead, the problem impacts to some degree all sounding sites that employ one of the most widely used types of radiosondes. We suspect that this bias may have first appeared near the start of the 1990s. The global nature of this bias and its potential impact on the climatic record has led us to investigate some of the implications of this error and its correction in the context of issues related to the Tropics and to the detection of climate change. Specifically, this paper investigates the impact of the humidity bias on the estimation of CAPE, CIN, and radiative fluxes in the Tropics using data from TOGA COARE.

## 2. The humidity correction

### a. Nature of the correction

The development of a correction procedure began when the Vaisala Corporation tested numerous radiosondes of varying age in the laboratory following the documentation of a dry bias in the data taken by their radiosondes during TOGA COARE. Engineers at Vaisala found that the error was caused by contamination of the polymer used as the dielectric in the capacitive relative humidity (RH) sensor. The error likely appeared in the dataset around 1990–91, when a change was made in the packaging procedure. The error was found to increase with the age of the radiosonde. For the H-type polymer RH sensor used in this analysis, the dry bias can be as large as 8%–10% at high humidities for sondes aged for one or more years.

The dry bias correction affects the entire sounding profile varying as a function of RH and temperature. A summary of the correction procedure can be found in Cole and Miller (1999). A manuscript that describes the error and correction procedure in greater detail is currently in preparation at the Atmospheric Technology Division of the National Center for Atmospheric Research (NCAR/ATD) and Vaisala Corporation (H. Cole, personal communication). The manuscript in prepara-

tion also discusses why some sites can have an apparent moist bias at times due to handling and storage of the radiosondes and how these soundings were corrected. This apparent moist bias problem did not arise in the data presented in this note. The correction scheme employed herein uses either radiosonde age or a prelaunch independent reference relative humidity measurement at the surface to account for the observed dry bias. The correction scheme also incorporates additional updated calibration information generated by Vaisala. Specifically, new information on the temperature dependence of the RH measurement has resulted in improved RH estimations at cold temperatures, as discussed in Miloshevich et al. (2000). Also, a new adjustment that corrects for a moist bias in the calibration at high humidities has been incorporated into the correction procedure. It slightly alters the RH values above 75% RH (up to 2% at 100% RH in the H-type polymer sensor).

The procedures developed at Vaisala were tested for physical plausibility using data taken during the TOGA COARE project, and a final correction scheme was implemented at NCAR/ATD. This scheme also included a correction for prelaunch sensor arm heating (Cole 1993). Sensor arm heating by solar radiation and its associated erroneous reduction of the RH measurement were found to be common in many daytime soundings in TOGA COARE due to the large values of solar insolation and the frequent occurrence of light winds. This error occurs when the ambient vapor pressure remains constant, but due to the sensor arm heating, it is referenced to an erroneously high saturation vapor pressure (from the sensor arm temperature), resulting in a lowered RH measurement. The ventilation obtained after the first minute of sonde ascent allows the sensor arm temperature to come to equilibrium with its environment. Therefore, the sensor arm heating has an affect over the first minute of the sounding ascent so that only the lowest 300 m of data are impacted.

### b. Dataset and magnitude of the correction

The humidity correction was employed for data taken from eight sounding sites during TOGA COARE (see Parsons et al. 1994). In this paper, we present an analysis of data taken aboard the three cruises of the research vessel (R/V) *Moana Wave* during TOGA COARE. The cruise dates were 11 November 1992–5 December 1992, 16 December 1992–11 January 1993, and 28 January 1993–13 February 1993 encompassing a total of 64 days at sea. During these cruises, soundings were launched four times daily. Data from the R/V *Moana Wave* were selected for several reasons, including the high-quality surface data taken by several sensing systems, a bias that was well within the range exhibited by the eight sites, and the location of the vessel near the center of the COARE measurement array.

The mean relative humidity profile for the three cruises and the vertical structure of the correction is presented

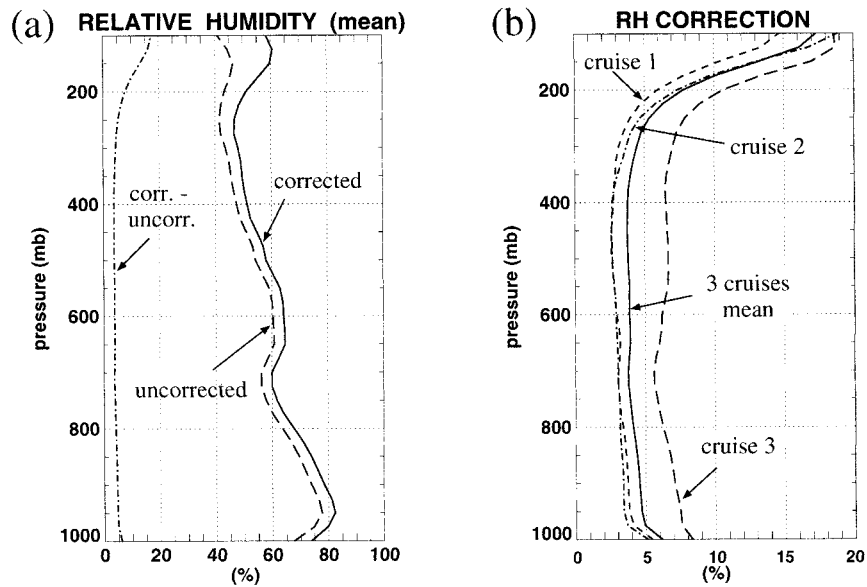


FIG. 1. Relative humidity: (a) mean profile average over the three cruises, corrected (solid line), uncorrected (dashed line), and the difference of corrected minus uncorrected (dashed-dotted line) and (b) magnitude of the average correction for the different cruises.

in Fig. 1a. A relatively uniform correction of 4% RH is observed over most of the troposphere. At the lowest levels, the correction is larger by 1%–2% due to the sensor arm heating problem discussed earlier. Above 300 hPa, the amplitude of the correction also increases significantly, reaching a maximum of more than 10% near 100 hPa, in agreement with Miloshevich et al. (2000). This large change in the upper troposphere RH is consistent with the dry bias found by Soden and Lanzante (1996) for radiosonde measurements of upper-tro-

pospheric water vapor over certain portions of the globe, as compared to satellite measurements. The vertical structure of this correction is very similar from one cruise to the other (Fig. 1b), although its magnitude varies significantly between cruises 1 and 2 on the one hand and cruise 3 on the other. For this last cruise, the correction is almost twice as large as the values for the first two. The corresponding mixing ratio correction (Fig. 2) is maximum in the lower layers, where values exceed  $1 \text{ g kg}^{-1}$ , with a gradual decrease with height.

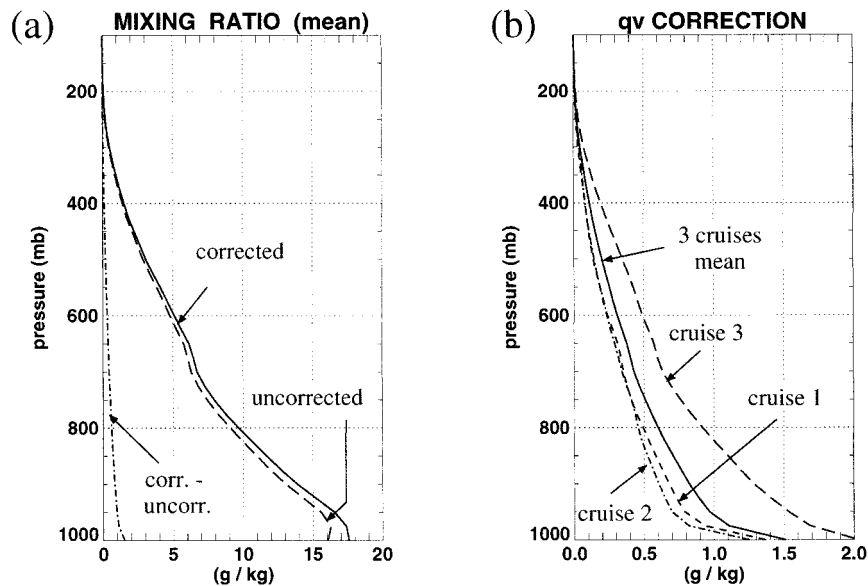


FIG. 2. Same as Fig. 1 but for mixing ratio.

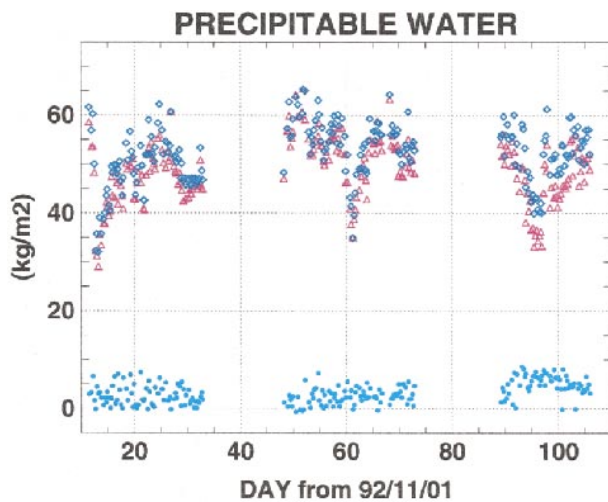


FIG. 3. Time series of precipitable water: uncorrected (pink triangles), corrected (blue diamonds), and the difference of corrected minus uncorrected (pale blue dots); time axis begins at 0000 UTC.

Fluctuations in the magnitude of the correction are further illustrated with the time series of precipitable water (PW) in Fig 3. The moisture correction almost always leads to larger values of PW, but the correction fluctuates widely from one sounding to the next. No clear relationship emerges between the level of humidity of the sounding and the magnitude of the correction, except for very moist cases (PW greater than  $60 \text{ kg m}^{-2}$ ) for which the correction is always weaker. Again, one can notice the increase of the correction for the last cruise.

### c. Discussion

At this point, a brief mention should be made as to how this correction compares to those derived using the correction procedure discussed in Lucas and Zipser (2000; hereafter LZ00). The philosophy of the LZ00 approach is largely based on attempting to diagnose the error in the dataset based on site-to-site differences and physical inferences. This empirical procedure aims at providing a first order ad hoc correction of the COARE dataset specifically. In the present paper, the nature of the correction procedure is very different, as it is based on the physics of the measurement technique and how the sensor behaved in detailed calibration tests. It is applied to COARE data; however, more generally, it aims at correcting the humidity bias obtained with Vaisala sondes. It is not surprising that the two techniques can lead to significantly different results.

In the LZ00 approach, a station bias was obtained for each sounding site, and this bias was applied as a constant from the second sounding point up to 700 hPa. Between 700 and 500 hPa, the station bias was applied as a function of height, with a linear interpolation that reached zero at 500 hPa. A second correction step was then undertaken where the data was corrected sounding

by sounding based on the difference between the surface and boundary layer humidity. This correction was uniformly applied in relative humidity as a function of height.

In practice, two factors should be kept in mind. Since the LZ00 dataset already included a sensor arm heating correction applied by NCAR/ATD, some height dependence to the mixing ratio difference between the corrected and uncorrected datasets will be present below 300 m. Also, this correction does not include the new calibration changes proposed by Vaisala, which moisten the upper levels. Another difference between the two methods is that LZ00 diagnose a sonde-by-sonde correction using the observed surface versus boundary layer moisture differences, while our approach uses the difference between a surface sensor and the radiosonde measurement prior to launch. The hypothesis that the surface-to-boundary layer moisture difference is known is based on theory and past observations over tropical oceans. We believe that the hypothesis is sound. In practice, however, the boundary layer depth can vary widely, especially following convective events where the mixed layer is initially removed (Zipser 1977). Therefore, the use of a fixed boundary layer depth in calculating moisture differences can be inappropriate, especially in cases where there is an extremely shallow boundary layer due to either convective outflow (e.g., Fig. 8 of Parsons et al. 1994) or nocturnal cooling over land.

Finally, the correction of the mixing ratio is constant, with height below 700 hPa in LZ00, while it decreases strongly with height in our dataset (Fig. 2). LZ00 use a correcting value of  $0.6 \text{ g kg}^{-1}$  for the R/V *Moana Wave*. This is below our estimate of the bias near the surface and slightly greater at 700 hPa. LZ00 also assume that the bias is constant with time up to 700 hPa, while our results indicate fluctuations of this bias with time (Figs. 1b and 2b).

### 3. Impact of the correction on calculations of convective instability

In the previous section, we showed that the largest correction to the water vapor mixing ratio was in the lower layers. The calculation of CAPE is extremely sensitive to the lower layer humidities, as noted by Crook (1996). Zipser and Johnson (1998) and LZ00 also noted that the errors in the humidity measurements made during TOGA COARE are likely to have a pronounced impact on the calculation of CAPE.

The difference between the corrected and uncorrected datasets can be seen in the histograms of the CAPE and CIN for the three cruises (Figs. 4 and 5), where the two datasets have strong qualitative differences. These corrected and uncorrected CAPEs and CINs were then averaged for each of the three cruises of the R/V *Moana Wave* (Fig. 6). In all cases, the CAPEs and CINs were calculated for parcel temperature and dewpoint corresponding to an average over the lowest 50 hPa. The

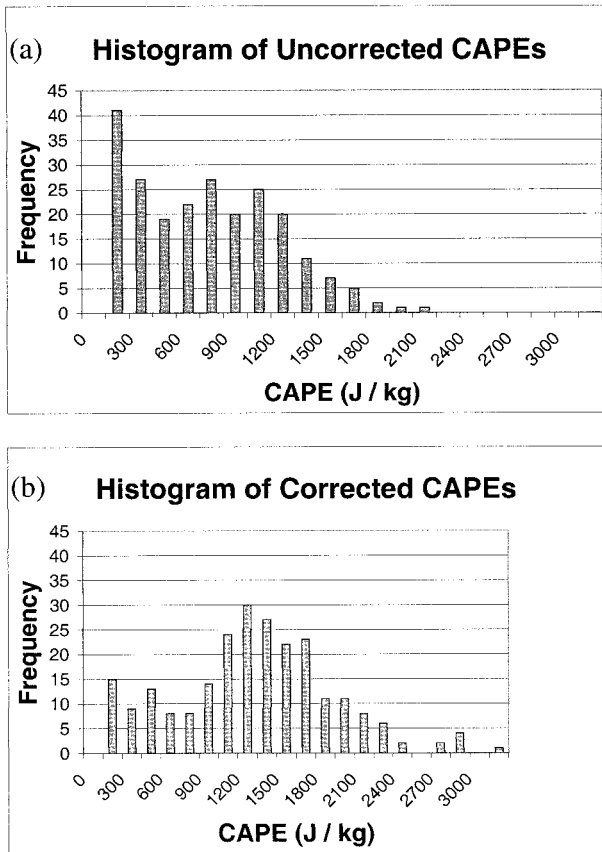


FIG. 4. Histogram of (a) uncorrected and (b) corrected CAPEs.

primary difference between the two datasets is that the uncorrected values are far more stable, with more CIN and less CAPE than the corrected counterparts. This general finding is consistent with the results of Zipser and Johnson (1999) and LZ00. The CAPE and CIN values of LZ00 (see their Table 7) lie between our corrected and uncorrected values, but somewhat closer to our corrected values. We suspect that this difference is primarily due to less moisture being added in the boundary layer in LZ00 than with our procedure.

From the mean uncorrected values of CAPE and CIN one would qualitatively interpret the atmosphere as becoming increasingly stable to deep convection over time as the CAPEs generally decrease and the CINs increase during the measurement period. The stability implied by the average uncorrected CIN is particularly noteworthy, with average values of  $-60 \text{ J kg}^{-1}$  for the first two cruises and of  $-120 \text{ J kg}^{-1}$  for the third cruise. To illustrate the physical meaning of these magnitudes, we will assume that the kinetic energy required for parcels in the mixed layer to overcome the observed CIN is supplied by vertical motions. With this assumption, unrealistically large updrafts of  $11 \text{ m s}^{-1}$  and nearly  $15.5 \text{ m s}^{-1}$  would be required to initiate or maintain convection during the two first cruises and third cruise, respectively.

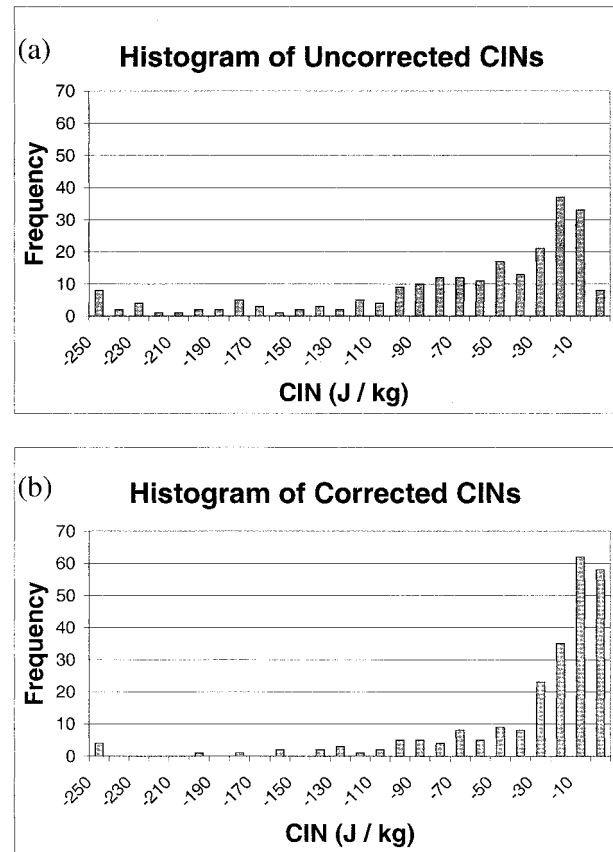


FIG. 5. Same as Fig. 4 but for CINs.

Our interpretation of the analyses of the radar datasets presented in the literature (e.g., Short et al. 1997; DeMott and Rutledge 1998; Rickenbach and Rutledge 1998) is that there is no plausible physical explanation for these relatively large CINs observed during the third cruise in the uncorrected datasets. In contrast, the CINs for the corrected data show that there is generally far less inhibition to convection and that the extreme CINs observed during the third cruise are greatly reduced. Thus, it is likely that the slow stabilization of the tropical atmosphere found in the uncorrected dataset is not physical but in reality results from a change in the dry bias with time, possibly due to an increase in the contamination as a radiosonde batch ages.

It is instructive to compare the uncorrected and corrected datasets with previous studies that use CAPE to study the stability of the atmosphere over the tropical oceans. LeMone et al. (1998) examined the environment in the vicinity of 20 convective systems observed with airborne measurements and found that the COARE convective environment had a range of CAPEs from 812 to  $1925 \text{ J kg}^{-1}$  with a mean value of  $1471 \text{ J kg}^{-1}$ . The CAPEs calculated by LeMone et al. (1998) were generally larger than those found during GATE [GARP (Global Atmospheric Research Project) Atlantic Tropical Experiment]. Using data from GATE, Barnes and

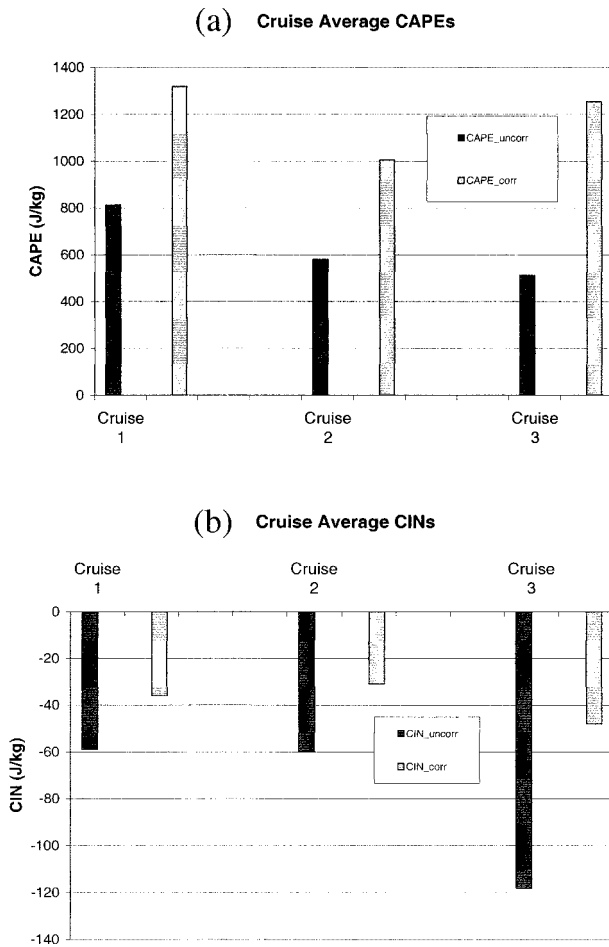


FIG. 6. Cruise average of (a) CAPEs and (b) CINs: uncorrected (black) and corrected (gray).

Sieckman (1984) found the average CAPEs for the so-called fast and slow moving convective lines to be 954 and 1138  $\text{J kg}^{-1}$ , respectively. The uncorrected average CAPEs for the R/V *Moana Wave* of between 511 and 812  $\text{J kg}^{-1}$  (Fig. 6a) are much smaller than reported by LeMone et al. (1998) and smaller than even the GATE results of Barnes and Sieckman (1984). In contrast, the average corrected CAPEs for the entire R/V *Moana Wave* dataset, which includes convective and suppressed periods, are generally larger than observed for GATE convection. The corrected CAPEs are within the range of the values found by LeMone et al. (1998) but on average smaller. In summary, from the average uncorrected data, one could wrongly infer that the basic state of the atmosphere of the COARE region is an environment where convection would be difficult to initiate and maintain and that the COARE region is more stable than GATE. The corrected dataset is more similar to the aircraft observations.

Several additional inferences can be drawn from the corrected dataset concerning the nature of the atmosphere over the tropical western Pacific. First, we find

that the CAPEs are within or exceed the range found by LeMone et al. (1998) for over three-quarters of the sampled population (Fig. 4b). Thus, the most common situation for the atmosphere over the tropical western Pacific during TOGA COARE appears to be at least as convectively unstable as the atmosphere was found to be in the vicinity of active deep convection. From the corrected CIN in Fig. 5b, we can conclude that the most common situation over the warm pool is to have CINs less than  $-10 \text{ J kg}^{-1}$  so that convection can be easily triggered and maintained. For these smaller CINs, it seems likely that local variations in the sea surface temperature (SST) or in the temperature at the top of the boundary layer will induce regions where CIN vanishes and convection is initiated. If convection is initiated in these common environments of small inhibition, gust fronts can then force parcels to their level of free convection, and convection can be maintained. LeMone et al. (1998) did not find any environments ahead of convective systems where the CIN was stronger than  $-25 \text{ J kg}^{-1}$ . In our dataset, “stable” values of CIN near or stronger than  $-30 \text{ J kg}^{-1}$  were found for only about 25% of the sampled population, again indicating that the atmosphere during COARE is typically near a threshold where convection can be easily initiated or at least maintained. Since the LeMone et al. (1998) study was restricted to environments in the vicinity of deep convection systems, one can conclude that the “typical” environment, as represented by this one site, has similar CAPEs and CINs, as occurs when organized systems are present.

Our finding of a tropical atmosphere over the COARE region typically being near the convective threshold is similar not only to the LeMone et al. (1998) aircraft study, but also confirms the results of Raymond (1995). While our ground-based approach has the disadvantage of relying on a correction procedure, it does provide a larger sample size than employed in those airborne studies. Raymond (1995), for example, used 44 aircraft soundings to conclude that the typical state of the atmosphere over this region is quite close to the threshold for convection. The previously mentioned radar studies also support the thermodynamic interpretation of a convectively active region, as periods without some form of deep convection are relatively rare over the warm pool.

The uncorrected dataset leads one to a different impression of the tropical atmosphere. The differences in CAPE and CIN are not limited to changes in the mean values and the distribution as the time rate of change of these quantities is also impacted. This time variation is used as a closure assumption in convective parameterizations and in attempting to understand the basic behavior of the tropical atmosphere (e.g., Zhang and Chou 1999). Time series of the CAPE and CIN for the third cruise of the R/V *Moana Wave* are shown in Fig. 7. From this figure, it is evident that the short-term variation between the uncorrected and corrected datasets

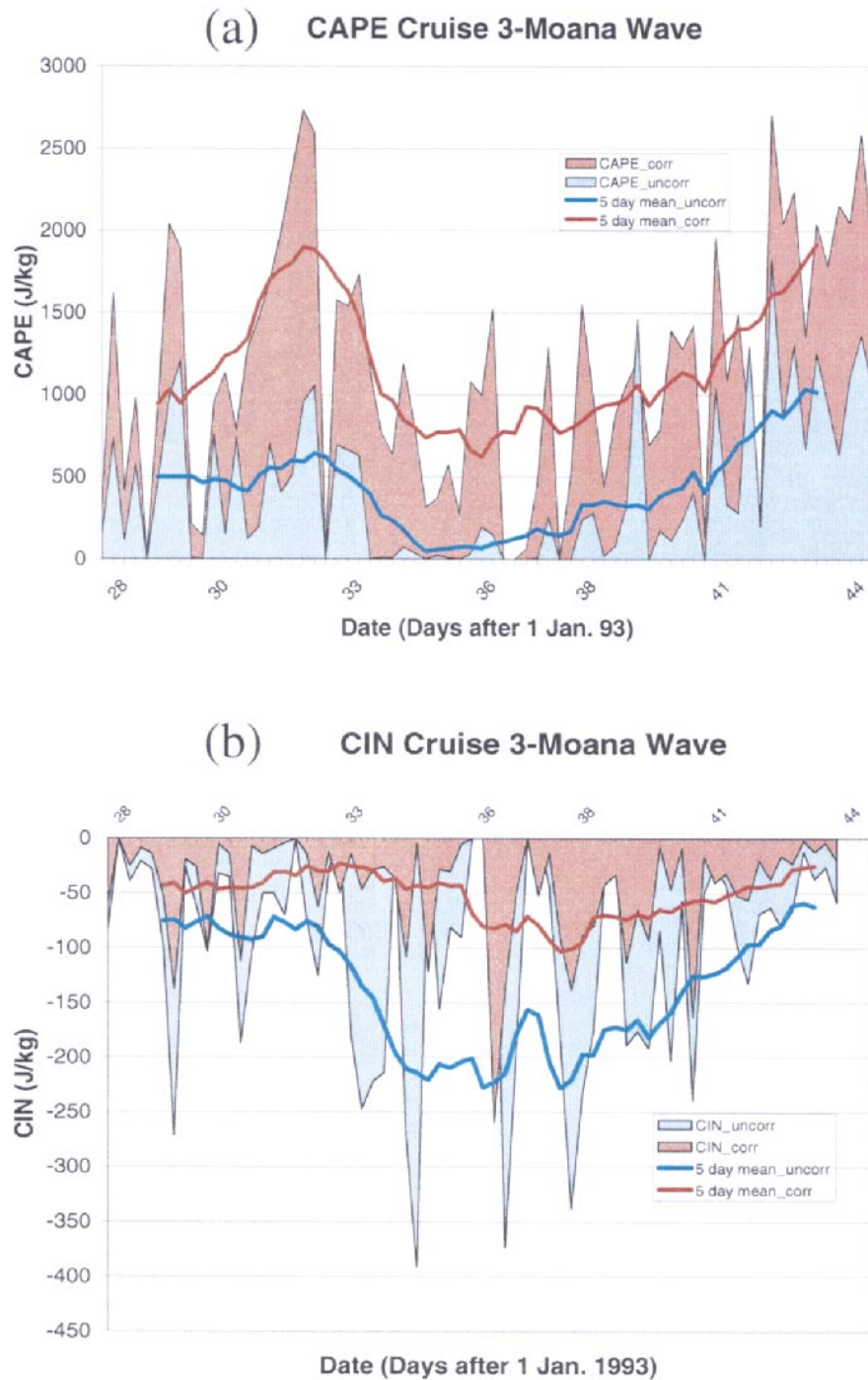


FIG. 7. Time series of (a) CAPEs and (b) CINs for cruise 3; the time sampling is 6 h, solid lines correspond to 5-day mean uncorrected (blue line) and corrected (red line) values.

is quite different. This difference in variation is due to linking the sounding humidity to the measurement at the surface, which corrects the dry bias and also reduces any sonde-to-sonde variance. Parsons et al. (1999) also noted that the diurnal cycle was modified as a result of the correction procedure. Some of the differences in the

time rate of change of the CAPE and CIN are reduced through time averaging. However, there are still significant differences in the time rate of change of the five-day running mean CAPE and CIN time series between the corrected and uncorrected datasets (Fig. 7, solid lines).

This is particularly obvious between days 29 and 32, with a CAPE increase for the corrected dataset only, and between days 32 and 35, with a decrease of the CIN being evident only in the uncorrected dataset. Thus for many purposes, previous studies that employ the TOGA COARE sounding dataset without the bias correction should be treated with a degree of caution that varies with how much the calculations and results depend upon the vertical profile of water vapor.

#### 4. Impact of the correction on radiative fluxes

The impact of the RH correction is not limited to atmospheric thermodynamics. Water vapor also plays a very important role in the earth radiation budget (Spencer and Braswell 1997) and in global climate change estimates (Lindzen 1990; Rind 1998). For instance, global climate change involves a modification of the radiative forcing of the order of a few watts per square meter (mainly related to the atmospheric CO<sub>2</sub> increase), but the actual modification of radiative fluxes might be larger, in particular because of a significant water vapor positive feedback (e.g., Raval and Ramanathan 1989). In this section, we investigate the changes in the radiative fluxes that occur as a result of the RH bias correction.

##### a. Radiative calculation

The radiative calculations were performed with a stand-alone version of the radiation model used in the National Center for Atmospheric Research (NCAR) Community Climate Model (CCM) (Kiehl et al. 1996, 1998). In this model, the longwave (LW) radiation is treated with a broadband technique. The shortwave (SW) radiation is calculated with a delta-Eddington approximation, with 18 spectral intervals (Briegleb 1992). For cloudy columns calculations, the scheme requires information about the cloud fraction, cloud water mixing ratio, and effective radius at each vertical level. Clouds are treated as gray bodies in the LW, with an emissivity parameterized as a function of cloud liquid and/or ice water paths. Cloud SW optical properties follow the parameterization of Slingo (1989), the coefficients for ice being based on Ebert and Curry (1992). The surface albedo follows Briegleb (1992) for the ocean; surface emissivity equals 0.99, and the SST is fixed to 29.5°C.

Among the ensemble of soundings collected on the R/V *Moana Wave*, only those reaching 100 hPa are retained, resulting in 219 soundings being used in this analysis. The soundings were interpolated on a 25 hPa vertical grid between 1000 and 100 hPa for the radiation calculations. Above the 100 hPa level, 6 additional layers were added up to 1 hPa for radiation computations but without any modification of moisture at those levels. The modification of radiative fluxes induced by the correction of water vapor profiles was not very sensitive

to the vertical resolution or to the relative humidity assumptions above 100 hPa.

Calculations were performed assuming either clear sky or cloudy conditions. Temperature and moisture data can be used directly for the computation of radiative fluxes assuming clear sky conditions. However, because of the very large modulation of radiation by clouds over the COARE area, a more realistic picture of the impact of the water vapor correction is obtained when clouds are included in the calculations. Indeed, these calculations show the greatest sensitivity to assumptions related to the cloud field. The main objective of this study, however, is not to get the true cloud fields and radiative properties for each sounding, but rather, a rough estimate of the probable cloud field to assess the likely impact of the error and its correction. Thus, some relatively crude assumptions were used to define a cloud field.

For each sounding, a vertical profile of the cloud field, including vertical profiles of cloud fraction, cloud water content, and effective radius, is diagnosed. Then, this two-dimensional cloud field, a function of time and height, is used for the radiative calculations, with uncorrected and corrected moisture profiles. This framework allows us to isolate the radiative impact of only the changes in the water vapor field for cloudy conditions.

In our calculation with clouds, the cloud fraction was diagnosed as a function of the corrected relative humidity for each layer. The RH with respect to liquid water (to ice) was considered for temperatures greater (less) than 0°C (−23°C). For intermediate or “mixed phase” temperatures, the RH was interpolated in the same way as in the European Centre for Medium-Range Weather Forecasts (ECMWF) model (Simmons et al. 1999). When the relative humidity is larger than a given threshold value, the level is assumed to be cloudy. A threshold value of 90% was used above 800 hPa. Below that height, a slightly smaller value (87%) was adopted. (A comparison between simulated and observed radiative fluxes suggests that a value of the threshold that is constant in the vertical leads to a relative underestimation of low clouds.) The cloud water path (CWP) was expressed as a function of height, as in the cloud parameterization of the NCAR CCM version 2 (Kiehl et al. 1994). For each vertical level it is given by  $CWP = \int \rho_0 e^{-z/h_c} dz$ , where  $\rho$  is the cloud water density and  $z$  the height above the surface,  $\rho_0$  is fixed to 0.18 g m<sup>−3</sup> and  $h_c$  is a cloud water scale height expressed as  $h_c = A + B \cos^2 \alpha$ , with  $A = 1080$  m,  $B = 2000$  m, and  $\alpha$  is the latitude. Finally, the effective radius is fixed up to 10 microns for liquid droplets and varying between 10 and 30 microns for ice crystals (Kiehl et al. 1994).

In the following, we focus on radiative fluxes (noted  $\phi$ ) at the TOA and at the surface (SRF) in the LW and the SW range. Upward and downward fluxes will be noted  $\phi^\uparrow$  and  $\phi^\downarrow$ , respectively. Mean values of these fluxes, derived using previous assumptions about the cloud field, are summarized in Table 1. For each vertical

TABLE 1. Mean radiative fluxes at the TOA and surface: derived from various observations for the 4-month IOP over the IFA (Krueger and Burks 1998) and diagnosed for the three cruises.

	Albedo TOA (unitless)	$\phi^{\downarrow\text{SW}_{\text{SRF}}}$ ( $\text{W m}^{-2}$ )	$\phi^{\downarrow\text{LW}_{\text{SRF}}}$ ( $\text{W m}^{-2}$ )	$\phi^{\uparrow\text{LW}_{\text{TOA}}}$ ( $\text{W m}^{-2}$ )
Obs for IOP IFA mean	0.228–0.285	208–49	417–42	215–20
Three-cruise mean estimation	0.29	233	430	208

column, SW fluxes were computed at the actual time when the sounding was launched (0, 6, 12, or 18 h UTC). Thus, no diurnal averaging was performed. However, when averaged over the whole dataset, the net SW downward flux at the TOA  $\phi^{\downarrow\text{SW}_{\text{TOA}}}$  is within 5% of the average for this period. Mean values estimated from various observed datasets over the COARE IFA for the 4-month period are also presented (from Krueger and Burks 1998). This comparison is somewhat qualitative because the three-cruise mean corresponds to approximately one-half of the total period. However, it shows that the diagnosed radiative budget is quite reasonable. At the same time, the cloud radiative forcing (CRF) on the downward SW flux at the surface  $\phi^{\downarrow\text{SW}_{\text{SRF}}}$  is equal to  $94 \text{ W m}^{-2}$  on average ( $\text{CRF} = \phi^{\downarrow\text{SW}_{\text{SRF}}} - \phi^{\downarrow\text{SW}_{\text{SRF,clear}}}$ , with  $\phi^{\downarrow\text{SW}_{\text{SRF,clear}}}$  the downward SW radiative flux at the surface assuming clear sky conditions). This result is also very close to the values derived by Waliser et al. (1996) and Chou and Zhao (1997) for TOGA COARE. Thus, these comparisons suggest that the diagnosed cloud field is quite suitable for our purpose.

### b. Radiative impact

Since the correction of water vapor profiles is relatively uniform, the vertical structure of the atmospheric radiative heating rate is not dramatically changed—less than  $0.1 \text{ K day}^{-1}$  at any altitude. On average, it leads to an additional cooling of  $1.65 \text{ W m}^{-2}$  for the entire atmospheric column. This result is qualitatively similar to the discussions of Doherty and Newell (1984) on the radiative impact of scaling the water vapor mixing ratio profile by arbitrary values. The modification of TOA and SRF, noted  $\delta(\phi)$ , are summarized for the three cruises in Table 2. The mean values vary with each cruise. However, the impact is qualitatively always the same, as schematically summarized in Fig. 8a. Note that the net SW and LW fluxes are classically defined as  $\phi^{\downarrow\text{SW}} = \phi^{\downarrow\text{SW}} - \phi^{\uparrow\text{SW}}$  and  $\phi^{\uparrow\text{LW}} = \phi^{\uparrow\text{LW}} - \phi^{\downarrow\text{LW}}$ , respectively. Also,  $\phi^{\downarrow\text{SW}_{\text{TOA}}}$ ,  $\phi^{\uparrow\text{LW}_{\text{SRF}}}$  and  $\phi^{\downarrow\text{LW}_{\text{TOA}}}$  ( $=0$ ) are the same for both calculations with uncorrected or corrected moisture

profiles, so  $\delta(\phi^{\downarrow\text{SW}_{\text{TOA}}}) = -\delta(\phi^{\uparrow\text{SW}_{\text{TOA}}})$ ,  $\delta(\phi^{\uparrow\text{LW}_{\text{SRF}}}) = -\delta(\phi^{\downarrow\text{LW}_{\text{SRF}}})$ , and  $\delta(\phi^{\uparrow\text{LW}_{\text{TOA}}}) = \delta(\phi^{\downarrow\text{LW}_{\text{TOA}}}) = \delta(\text{OLR})$ , where OLR is the outgoing longwave radiation. Finally,  $\delta(\phi^{\uparrow\text{SW}_{\text{SRF}}}) \ll \delta(\phi^{\downarrow\text{SW}_{\text{SRF}}})$  because the sea surface albedo is very weak, so that  $\delta(\phi^{\downarrow\text{SW}_{\text{SRF}}}) \approx \delta(\phi^{\downarrow\text{SW}_{\text{SRF}}})$ . The moister atmosphere absorbs more incoming radiation, resulting in a decrease of the downward SW flux at the surface of the order of  $-0.79 \text{ W m}^{-2}$ . Because the ocean has a low albedo, the impact on the SW flux at the top of the atmosphere is quite weak. It is even weaker for clear sky conditions (Fig. 8b) because in that case, no shallow clouds with a high albedo are present to reflect the incoming solar radiation. In the LW, the impact is significant, both at the surface and TOA. The atmospheric greenhouse effect is increased for the corrected soundings, with an enhancement of the LW downward flux at the surface of  $2.85 \text{ W m}^{-2}$ , whereas the radiation lost to space at the TOA decreases by  $1.2 \text{ W m}^{-2}$ . At the surface, modification of SW and LW fluxes have an opposite sign, but the impact on the LW flux is larger, so that there is a net increase of the downward flux at the surface.

The impact of the cloud cover in these calculations is important (Fig. 8). In effect, the same computation assuming clear sky columns leads to the same qualitative effect but with a magnitude twice that of the cloudy conditions (Fig. 8b).

The modifications of radiative fluxes  $\delta\phi$  are very strongly correlated to the correction of precipitable water ( $\delta\text{PW}$ ) for cloudy (Fig. 9) and for clear sky (Fig. 10) calculations. This indicates that the most important parameter controlling the modification of radiative fluxes is the “homogeneous shift” over the whole tropospheric height, not the large increase of relative humidity in the upper levels. Clear sky conditions appear as the most dramatic (Fig. 10). Values of  $\delta\phi$  are almost linearly coupled to  $\delta\text{PW}$ . The larger slope corresponds to  $\phi^{\downarrow\text{LW}_{\text{SRF}}}$  (Fig. 10d): an increase of  $1 \text{ kg m}^{-2}$  leading approximately to a  $1.4 \text{ W m}^{-2}$  increase of  $\phi^{\downarrow\text{LW}_{\text{SRF}}}$ .

Except for the upward shortwave flux at the TOA (Fig. 9a), the diagnosed cloud field tends to partly shad-

TABLE 2. Modification of radiative fluxes ( $\text{W m}^{-2}$ ) induced by the moisture correction; the precipitable water increase ( $\text{kg m}^{-2}$ ) is also indicated.

	$\delta(\phi^{\uparrow\text{SW}_{\text{TOA}}})$	$\delta(\phi^{\downarrow\text{SW}_{\text{SRF}}})$	$\delta(\phi^{\downarrow\text{LW}_{\text{SRF}}})$	$\delta(\phi^{\uparrow\text{LW}_{\text{TOA}}})$	Precipitable water
Cruise 1	-0.23	-0.78	2.55	-1.29	2.69
Cruise 2	-0.19	-0.47	1.66	-0.85	2.51
Cruise 3	-0.22	-1.22	4.77	-1.55	5.11

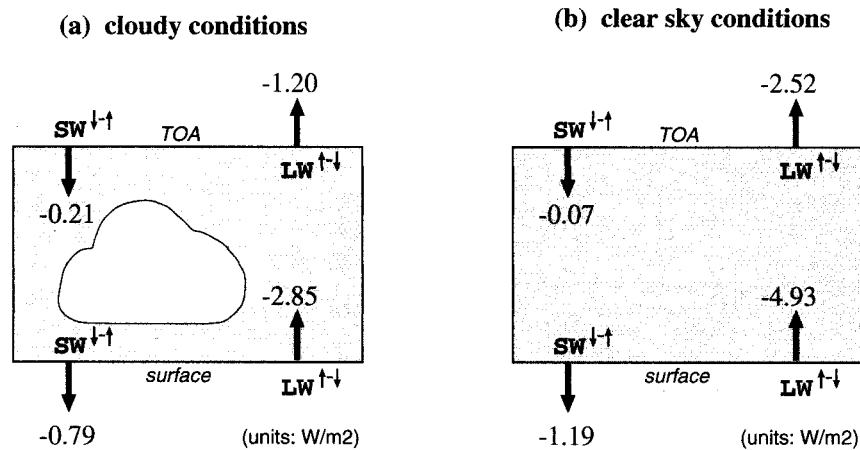


FIG. 8. Three-cruise mean radiative impact of the RH correction assuming (a) cloudy and (b) clear sky conditions; in (a), the same (two-dimensional) cloud field is used for both calculations, with the uncorrected and the corrected humidity profiles.

ow the impact of the moisture correction—it plays the same role when considering the impact of doubling  $\text{CO}_2$ . For a given value of  $\delta\text{PW}$ ,  $\delta\phi$  lies between 0 and the extreme clear sky case value. The scatter of  $\delta\phi$  for a given value of  $\delta\text{PW}$  is related to the type of cloud that is diagnosed, at first order to its height and optical depth. In short, when low-level optically thick clouds are present, the modification of the LW downward flux at the surface is smaller than for clear sky conditions, whereas  $\delta(\text{OLR})$  is almost the same. The opposite is found for high-level clouds such as cirrus. In the SW, diagnosed low-level clouds are responsible for the decrease of  $\phi_{\text{SWTOA}}^{\uparrow}$  for the moister atmosphere. Their albedo is much larger than the small albedo of the oceanic surface, so they induce more reflection of the solar radiation. The reflected radiation, in turn, experiences more atmospheric absorption in the moister atmosphere above the clouds before reaching the TOA. At the same time, high clouds partly reflect the incoming solar radiation. So the modification of  $\phi_{\text{SWSRF}}^{\downarrow}$  is weaker when high clouds are diagnosed.

Thus, the modification of radiative fluxes varies widely from one sounding to the other, primarily as a function of the precipitable water correction and the cloud cover. For an individual sounding, it can be as large as 5 and  $10 \text{ W m}^{-2}$  at the TOA and surface, respectively. On average, it is still of the order of  $2 \text{ W m}^{-2}$  at the surface (increasing the downward flux to the ocean) and  $1 \text{ W m}^{-2}$  at the TOA (decreasing the OLR). These values are in the same range as the radiative forcing due to the atmospheric  $\text{CO}_2$  increase from preindustrial times to present days (Schimel et al. 1996). Doubling  $\text{CO}_2$  in the present calculations leads to an  $1 \text{ W m}^{-2}$  increase of  $\phi_{\text{LWSRF}}^{\downarrow}$ . This moisture-induced modification of radiative fluxes is also larger than existing estimates of the indirect radiative forcing of aerosols, of the order of  $0.5 \text{ W m}^{-2}$ , with a large range of uncertainties (Boucher

1995). Thus, this modification of radiative fluxes appears as climatologically important.

Another implication of the humidity error is that a full atmospheric model would also predict differences in cloud cover given the differences between the corrected and uncorrected humidity profiles. This should result in a significant modification of radiative fluxes through the changes of the cloud cover. Indeed, with our simple representation of the cloud field, the increase of the cloud cover induced by the RH correction leads to modifications of the radiative fluxes of more than  $50 \text{ W m}^{-2}$  and  $10 \text{ W m}^{-2}$  in the SW and LW, respectively.

## 5. Conclusions

In this study, we have presented the impact of a correction of humidity measurements with radiosondes on estimations of CAPE, CIN, and radiative fluxes. The time series of radiosonde data collected on the R/V *Moana Wave* during the COARE experiment has been systematically analyzed. On average, the correction leads to an increase of relative humidity of several percent over the whole troposphere, with an additional increase in the upper troposphere. The correction exhibits a vertical structure that is quite similar from one sounding to another, but its magnitude, which depends in part on the age of the sonde, shows large fluctuations.

The impact on the CAPEs and CINs over the warm pool was dramatic due to the sensitivity of these quantities to the low-level moisture. When the correction is taken into account, it is clear that the environment over the warm pool is typically unstable to deep convection, with values of the CAPE and CIN similar to those values found in the vicinity of active deep convection by in situ aircraft measurements. From the uncorrected sounding data, one would erroneously conclude that it is very difficult to trigger convection over the COARE region.

## MODIFICATION OF RADIATIVE FLUXES : "CLOUDY SKY"

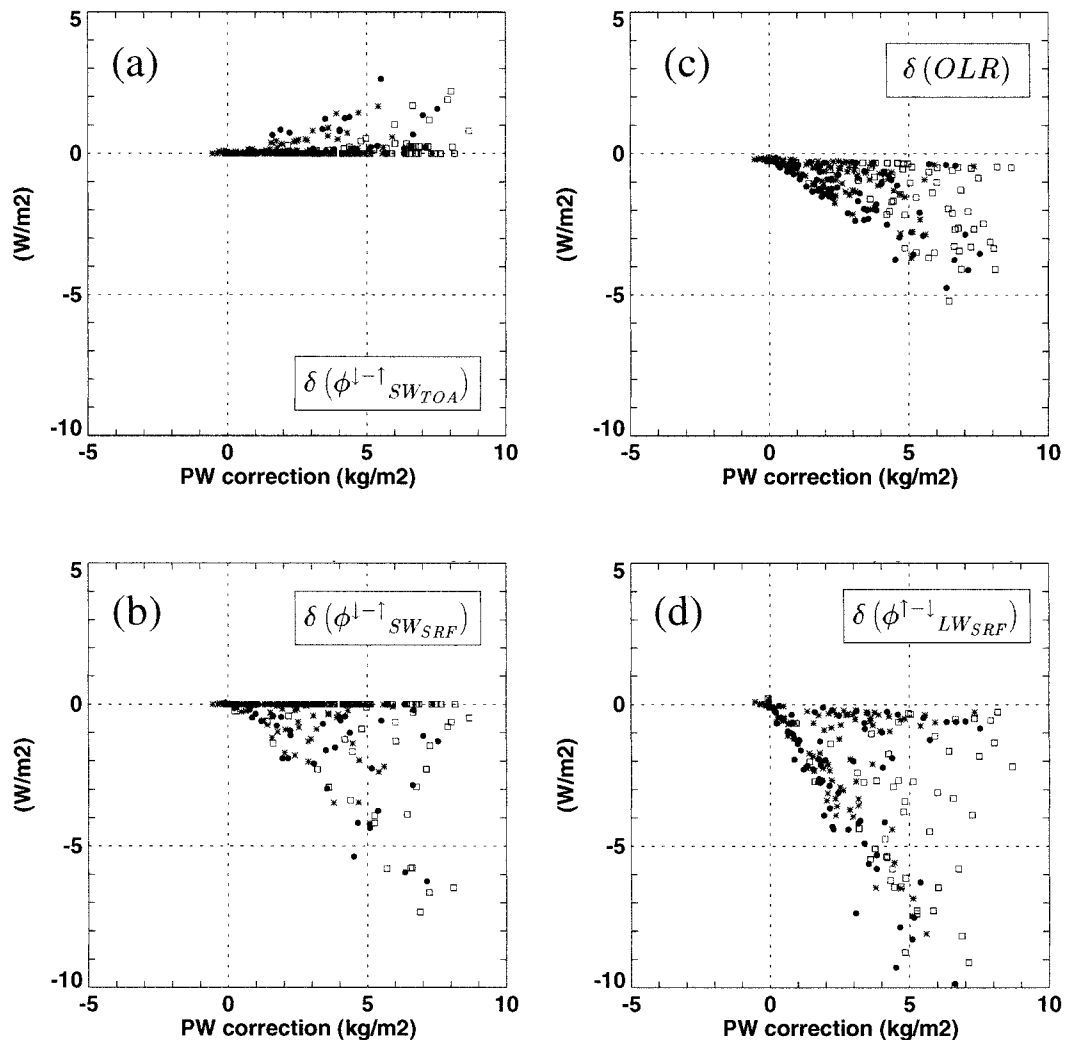


FIG. 9. Modification of radiative fluxes as a function of the precipitable water correction, at the TOA and at the surface, in the shortwave (a) and (b) and the longwave (c) and (d) for each of the 219 soundings assuming cloudy conditions; circles, stars, and squares identify cruises 1, 2, and 3 soundings, respectively.

Radiative calculations indicate that on average, the moisture correction induces a  $2 \text{ W m}^{-2}$  increase of the downward flux at the surface and a  $1 \text{ W m}^{-2}$  decrease of the OLR. These values are obtained under cloudy conditions. For clear sky conditions, the modification of radiative fluxes is almost twice as much. It has been found that for this specific moisture correction, modifications of radiative fluxes are strongly related to the precipitable water correction, and their magnitudes are controlled by the cloud fields. The mean bias and the sonde-to-sonde variations equal or exceed the accuracy required to answer many questions related to the radiative budget, questions that must be addressed in order to understand and predict climate change. It seems likely

that such a dry bias would hide any modifications of the atmospheric water vapor associated with the increase of greenhouse gases.

The implications of this error for COARE studies are not limited to the radiation budget and the calculation of CAPE and CIN. For example, it can be anticipated that this moisture correction may have a significant impact on COARE derived products that use sounding data, for example, large-scale budgets (e.g. Lin and Johnson 1996). In these budgets, a problem arises in the calculation of spatial gradients, as there are large site-to-site differences in the biases as demonstrated by Lucas and Zipser (2000). Thus, the error does not only impact the mean profiles but also the spatial gradients

## MODIFICATION OF RADIATIVE FLUXES : "CLEAR SKY"

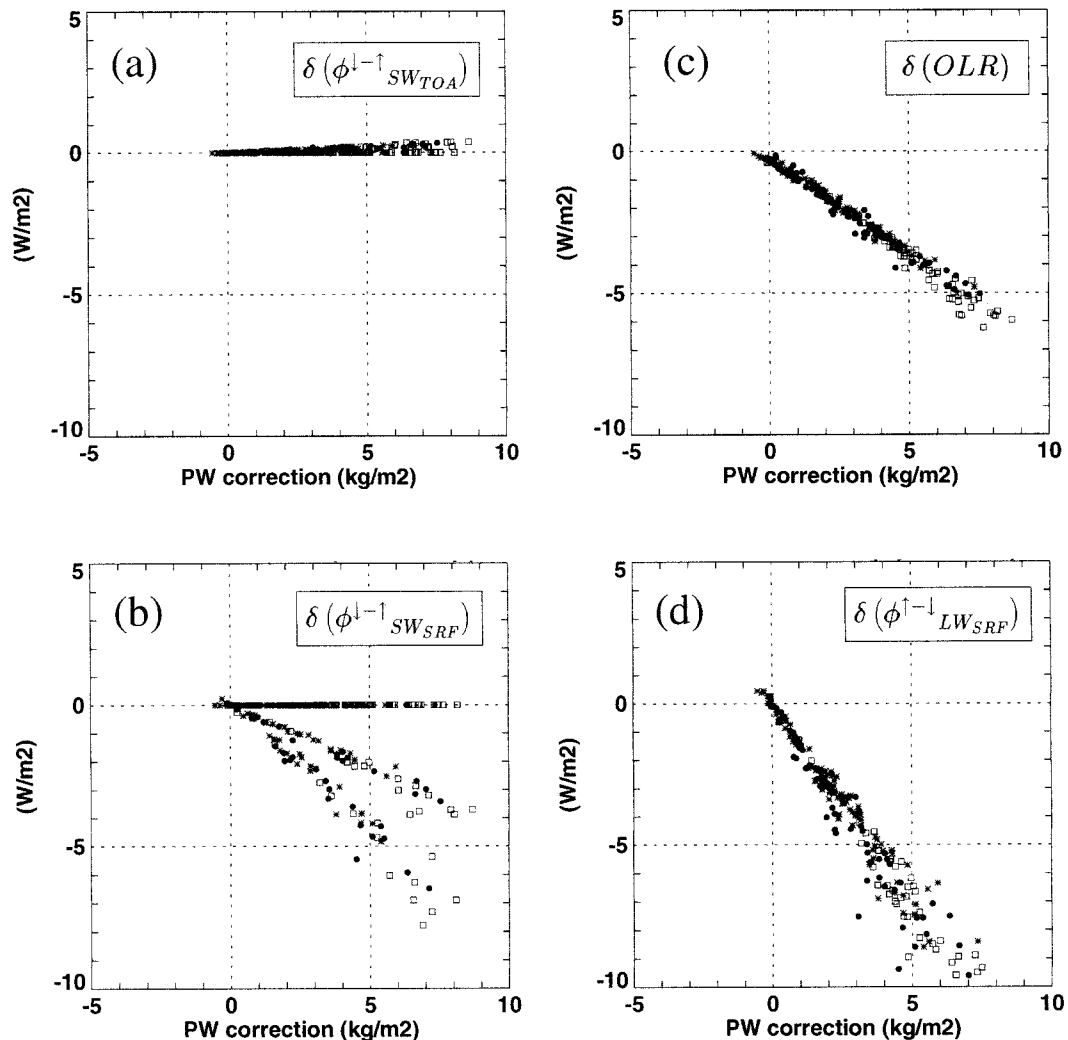


FIG. 10. Same as Fig. 9 except assuming clear sky conditions.

derived using objective analyses. While we do not doubt most of the scientific inferences drawn in Lin and Johnson (1996), there may be some quantitative changes in their analysis of the water vapor field. Hence, if these analyses are used for forcing single column and cumulus ensemble models (Moncrieff et al. 1997), there might be some changes in the simulations, especially in light of the sensitivity of single column models to initial conditions (Hack and Pedretti 2000).

We have used the COARE dataset to illustrate the scientific implications of this error. This correction is not restricted to COARE measurements, however, but extends to a very large number of radiosonde measurements taken during this decade. The dry bias is probably the most pronounced in North America, as H-Humicap sondes are more widely used there. It can also be ex-

pected that the magnitude of the dry bias is not as large as during COARE because many synoptic stations do not store radiosondes for long periods, thus reducing the magnitude of the error (T. Lane, personal communication). Clearly, further investigation is needed if one wants to get a complete picture of the problem on a global scale.

Weather forecast models, which directly ingest sounding data in their analysis, should exhibit a sensitivity to this sudden moisture increase if the sounding data are not rejected in the data assimilation processes. In particular, many existing convective schemes assume a CAPE closure, relating the intensity of convection to the rate of CAPE variation. In regard to the large CAPE modification, this correction should significantly impact the simulated convective activity. Indeed, Johnson and

Ciesielski (2000) show that rainfall biases of NCEP and ECMWF reanalysis over the COARE region can be partly explained in terms of the moisture bias of the measurements by radiosondes manufactured by different vendors. In addition, cloud parameterizations in general circulation models usually relate the cloud fraction to the relative humidity. This moisture correction will act to enhance the cloud cover, especially at high altitude, because of the large increase of relative humidity in the upper troposphere. These additional high clouds, in turn, may have a strong impact on the model radiative budget.

The discovery of an error in the measurement of humidity with Vaisala radiosondes led to a significant improvement of the physics of the measurement technique. Similarly, it can be expected that this moisture correction will also contribute to an enhancement of our current understanding of the atmosphere.

*Acknowledgments.* This work was supported by DOE ARM grant DE-AI0297ER62359 and TOGA COARE grants from NSF NSF01. We would, of course, like to acknowledge the technical staff who made the TOGA COARE measurements possible. Discussions with H. Cole, D. Carlson, J.-H. Wang, R. Johnson, C. Fairall, and B. Lesht have been very beneficial. A. Paukkunen and T. Laine are acknowledged on the development and implementation of the correction procedure. We would like to acknowledge the numerous investigators and forecasters who noted problems with the radiosonde humidity measurements during TOGA COARE, which partially led to the development of this correction procedure. In particular, we acknowledge the efforts of P. Ciesielski, R. Johnson, P. LeMone, C. Lucas, and E. Zipser whose research efforts clearly articulated the need for this correction. We also thank L. Verstraete, who kept and archived unused sondes from the COARE project, which upon discovery led to the bias in calibration chamber tests. Finally, we thank C. Zender, who provided the radiative code, and H. Cole, D. Carlson, P. LeMone, and two anonymous reviewers for helpful suggestions concerning the manuscript. Careful editing of the manuscript by C. Darnell is also acknowledged.

#### REFERENCES

- Barnes, G., and K. Sieckman, 1984: The environment of fast- and slow-moving tropical mesoscale convective cloud lines. *Mon. Wea. Rev.*, **112**, 1782–1794.
- Barr, A. G., and A. K. Betts, 1997: Radiosonde boundary layer budgets above a boreal forest. *J. Geophys. Res.*, **102**, 29 205–29 212.
- Boucher, O., 1995: GCM estimate of the indirect aerosol forcing using satellite-retrieved cloud droplet effective radii. *J. Climate*, **8**, 1403–1409.
- Briegleb, B., 1992: Delta-Eddington approximation for solar radiation in the NCAR Community Climate Model. *J. Geophys. Res.*, **97**, 7603–7612.
- Chou, M.-D., and W. Zhao, 1997: Estimation and model validation of surface solar radiation and cloud radiative forcing using TOGA COARE measurements. *J. Climate*, **10**, 610–620.
- Colby, F. P. J., 1983: Effects of boundary-layer modification on the initiation of convection during AVE-SESAME, 1979. *Mesoscale Meteorology—Theories, Observations, and Models*, D. K. Lilly and T. Gal-Chen, Eds., NATO ASI Series C, Vol. 114, Kluwer Academic, 709–710.
- Cole, H., and E. Miller, 1995: A correction for low-level radiosonde temperature and relative humidity measurements. Preprints, *Ninth Symp. on Meteorological Observations and Instrumentation*, Charlotte, NC, Amer. Meteor. Soc., 32–36.
- , and —, 1999: Correction and re-calculation of humidity data from TOGA COARE radiosondes and development of humidity correction algorithms for global radiosondes data. *Proc. WCRP COARE-98 Conf.*, WCRP 107, WMO/TD-940, Boulder, CO, 139–141.
- Crook, N. A., 1996: Sensitivity of moist convection forced by boundary layer processes to low-level thermodynamic fields. *Mon. Wea. Rev.*, **124**, 1767–1785.
- Dabberdt, W. F., and T. W. Schlatter, 1996: Research opportunities from emerging atmospheric observing and modeling capabilities. *Bull. Amer. Meteor. Soc.*, **77**, 305–323.
- DeMott, C. A., and S. Rutledge, 1998: The vertical structure of TOGA COARE convection. Part I: Radar echo distributions. *J. Atmos. Sci.*, **55**, 2730–2747.
- Doherty, G., and R. Newell, 1984: Radiative effects of changing atmospheric water vapour. *Tellus*, **36B**, 149–162.
- Ebert, E., and J. A. Curry, 1992: A parameterization of ice cloud optical properties for climate models. *J. Geophys. Res.*, **97**, 3831–3836.
- Emanuel, K., and Coauthors, 1995: Report of the first Prospectus Development Team of the U.S. Weather Research Program to NOAA and the NSF. *Bull. Amer. Meteor. Soc.*, **76**, 1194–1208.
- Gutzler, D. S., 1993: Uncertainties in climatological tropical humidity profiles: Some implications for estimating the greenhouse effect. *J. Climate*, **6**, 978–982.
- Hack, J. J., and J. A. Pedretti, 2000: Assessment of Solution Uncertainties in Single-Column Modeling Frameworks. *J. Climate*, **13**, 352–365.
- Harries, J. E., 1997: Atmospheric radiation and atmospheric humidity. *Quart. J. Roy. Meteor. Soc.*, **123**, 2173–2186.
- Johnson, R. H., and P. E. Ciesielski, 2000: Rainfall and Radiative Heating Rates from TOGA COARE Atmospheric Budgets. *J. Atmos. Sci.*, **57**, 1497–1514.
- Kiehl, J. T., J. J. Hack, and B. P. Briegleb, 1994: The simulated earth radiation budget of the NCAR CCM2 and comparisons with the Earth Radiation Budget Experiment (ERBE). *J. Geophys. Res.*, **99**, 20 815–20 827.
- , —, G. B. Bonan, B. A. Boville, D. L. Williamson, and P. J. Rasch, 1998: The National Center for Atmospheric Research Community Climate Model: CCM3. *J. Climate*, **11**, 1131–1149.
- Krueger, S. K., and J. E. Burks, 1998: Radiative fluxes and heating rates during TOGA COARE over the intensive flux array. *Proc. Eighth Atmospheric Radiation Measurement (ARM) Science Team Meeting*, Tucson, AZ, Department of Energy, 400–402.
- LeMone, M., E. Zipser, and S. Trier, 1998: The role of environmental shear and thermodynamic conditions in determining the structure and evolution of mesoscale convective systems during TOGA COARE. *J. Atmos. Sci.*, **55**, 3493–3518.
- Lin, X., and R. H. Johnson, 1996: Heating, moistening, and rainfall over the western Pacific warm pool during TOGA COARE. *J. Atmos. Sci.*, **53**, 3367–3383.
- Lindzen, R., 1990: Some coolness concerning global warming. *Bull. Amer. Meteor. Soc.*, **71**, 288–299.
- Lucas, C., and E. J. Zipser, 2000: Environmental variability during TOGA COARE. *J. Atmos. Sci.*, **57**, 2333–2350.
- Miloshevich, L. M., H. Vömel, A. Paukkunen, A. J. Heymsfield, S. J. Oltmans, 2000: Characterization and correction of relative humidity measurements from Vaisala RS80-A radiosondes at cold temperatures. *J. Atmos. Oceanic Technol.*, in press.
- Moncrieff, M., S. Krueger, D. Gregory, J.-L. Redelsperger, and W.-K. Tao, 1997: GEWEX Cloud System Study (GCSS) Working

- Group 4: Precipitating convective cloud systems. *Bull. Amer. Meteor. Soc.*, **78**, 831–844.
- Parsons, D., and Coauthors, 1994: The integrated sounding system: Description and preliminary observations from TOGA COARE. *Bull. Amer. Meteor. Soc.*, **79**, 553–567.
- , K. Yoneyama, and J.-L. Redelsperger, 2000: The evolution of the atmosphere–ocean systems over the tropical western Pacific following the arrival of a dry intrusion. *Quart. J. Roy. Meteor. Soc.*, **126**, 517–548.
- Raval, A., and V. Ramanathan, 1989: Observational determination of the greenhouse effect. *Nature*, **342**, 758–761.
- Raymond, D. J., 1995: Regulation of moist convection over the west Pacific warm pool. *J. Atmos. Sci.*, **52**, 3945–3959.
- Rickenbach, T. M., and S. Rutledge, 1998: Convection in TOGA COARE: Horizontal scale, morphology, and rainfall production. *J. Atmos. Sci.*, **55**, 2715–2729.
- Rind, D., 1998: Just add water vapor. *Science*, **281**, 1152–1153.
- Schimel, D., and Coauthors 1995: Radiative forcing of climate change. *Climate Change 1995: The Science of Climate Change*, J. T. Houghton et al., Eds., Cambridge University Press, 65–131.
- Short, D. A., P. A. Kucera, B. S. Ferrier, J. C. Gerlach, S. A. Rutledge, and O. W. Thiele, 1997: Shipboard radar rainfall patterns within the TOGA COARE IFA. *Bull. Amer. Meteor. Soc.*, **78**, 2817–2836.
- Simmons, A. J., A. Untch, C. Jakob, P. Kallberg, and P. Uden, 1999: Stratospheric water vapour and tropical tropopause temperatures in ECMWF analyses and multi-year simulations. *Quart. J. Roy. Meteor. Soc.*, **125**, 353–386.
- Slingo, A., 1989: GCM parameterization for the short-wave radiative properties of water clouds. *J. Atmos. Sci.*, **46**, 1419–1427.
- Smith, T. L., and S. G. Benjamin, 1993: Impact of network wind profiler data on a 3-h data assimilation system. *Bull. Amer. Meteor. Soc.*, **74**, 801–807.
- Soden, B., and J. Lanzante, 1996: An assessment of satellite and radiosonde climatologies of upper-tropospheric water vapor. *J. Climate*, **9**, 1235–1250.
- Spencer, R. W., and W. D. Braswell, 1997: How dry is the tropical free troposphere? Implications for global warming theory. *Bull. Amer. Meteor. Soc.*, **78**, 1097–1106.
- Waliser, D., W. D. Collins, and S. P. Anderson, 1996: An estimate of the surface shortwave cloud forcing over the western Pacific during TOGA COARE. *Geophys. Res. Lett.*, **23**, 519–522.
- Weckwerth, T. M., V. Wulfmeyer, R. M. Wakimoto, R. M. Hardesty, J. W. Wilson, and R. M. Banta, 1999: NCAR/NOAA lower tropospheric water vapor workshop. *Bull. Amer. Meteor. Soc.*, **80**, 2339–2357.
- Zhang, C., and M.-D. Chou, 1999: Variability of water vapor, infrared radiative cooling, and atmospheric instability for deep convection in the equatorial western Pacific. *J. Atmos. Sci.*, **56**, 711–723.
- Zipser, E. J., and R. H. Johnson, 1998: Systematic errors in radiosonde humidities a global problem? Preprints, *10th Symp. on Measurements, Observations and Instrumentation*, Phoenix, AZ, Amer. Meteor. Soc., 72–73.